

# Cross-Modality Fusion Transformer for Multispectral Object Detection

Fang Qingyun, Han Dapeng, Wang Zhaokui, *Member, IEEE*

**Abstract**—Multispectral image pairs can provide the combined information, making object detection applications more reliable and robust in the open world. To fully exploit the different modalities, we present a simple yet effective cross-modality feature fusion approach, named Cross-Modality Fusion Transformer (CFT) in this paper. Unlike prior CNNs-based works, guided by the transformer scheme, our network learns long-range dependencies and integrates global contextual information in the feature extraction stage. More importantly, by leveraging the self attention of the transformer, the network can naturally carry out simultaneous intra-modality and inter-modality fusion, and robustly capture the latent interactions between RGB and Thermal domains, thereby significantly improving the performance of multispectral object detection. Extensive experiments and ablation studies on multiple datasets demonstrate that our approach is effective and achieves state-of-the-art detection performance. Our code and models will be released soon at <https://github.com/DocF/multispectral-object-detection>.

**Index Terms**—Cross-modality, feature fusion, multispectral object detection, transformer.

## I. INTRODUCTION

IN real-world object detection applications, the environment is often open and dynamic, requiring models and algorithms to deal with the challenges caused by openness, such as rain, fog, occlusions, poor lighting, low resolution, etc. It is difficult for an algorithm that uses only visible-band sensor data to achieve high accuracy under these conditions. Hence, the multispectral imaging technology is gradually being adopted, given its ability to provide the combined information coming from multispectral cameras e.g., visible and thermal. And by fusing the complementary of different modalities, the perceptibility, reliability, and robustness of detection algorithms can be further improved.

Recent advances in convolutional neural networks (CNNs), more specifically, two-stream CNN-based detectors, have encouraged detection performance in the field of multispectral object detection[1–9]. In addition, some challenging multispectral datasets, e.g. FLIR[10], LLVIP[11], VEDAI[12], have also driven the continuous development of this field.

Figure 1 shows some examples to illustrate the advantages of multispectral images over visible-only or thermal-only images under different conditions. However, the exploitation of multispectral data will raise some new questions: How to integrate the representations to fully make use of the inherent complementary between different modalities? And how to design an effective cross-modality fusion mechanism for maximum performance gain?

In the prior works, no matter how to design the modal fusion mechanism, they are all mostly based on deep convolutional



Fig. 1. Visible-infrared paired examples from LLVIP. The paired images in the first row are captured in nighttime traffic scenes. Compared with the visual image on the left, the thermal image on the right can capture the clearer contours of pedestrians under insufficient illumination conditions. Besides, the thermal image also captures pedestrians obscured by a pillar. The paired images in the second row are captured in daytime traffic scenes. During well-lit daytime, the visual image has more details, such as edges, textures, and colors, than thermal images. With these details, we can easily find the driver hidden in the motor tricycle, which is difficult to find in the thermal image. Zoom in to see details.

neural networks[1, 3, 5, 7, 8]. There is considerable literature that has proven that CNNs can have strong representation learning capabilities within a single intra-modal reasoning [13–18], especially for visual modality. However, it is non-trivial to extend them to cross-modality fusion or modality interaction to fully exploit the inherent complementary. The convolution operator of CNNs can be regarded as a non-fully connected graph with each spatial position in the feature maps as a node. Since the convolution operator has a non-global receptive field, the information is only fused in a local area. In contrast, the self attention operator of transformer [19] can be regarded as a fully connected graph, so it can learn long-range dependencies and its receptive field can be global. For the above considerations, we propose a novel and effective multispectral fusion approach, which is called *Cross-Modality Fusion Transformer* (CFT), to integrate global contextual information of different modalities in the feature extraction backbone. And to the best of our knowledge, this is the first work adopting the transformer for multispectral object detection.

**Contributions:** (1) We introduce a new and powerful two-stream backbone which enhances one modality from another

modality under the guidance of the transformer scheme. (2) We propose a simple yet effective CFT module, and give theoretical insights into it, showing that the CFT module simultaneously fuses the intra-modality and inter-modality features; (3) Experimental results achieve the state-of-the-art performance on three public datasets, which confirm the effectiveness of the proposed approaches.

## II. RELATE WORK

Fusing the feature of two modalities is the core problem in multispectral object detection, which can be described as

$$\mathbf{F}_{Fused} = \mathcal{F}(\mathbf{F}_R, \mathbf{F}_T), \quad (1)$$

where  $\mathbf{F}_R$  denotes the RGB modality features and  $\mathbf{F}_T$  denotes the Thermal modality features.  $\mathbf{F}_{Fused}$  indicates the fused features, and  $\mathcal{F}(\mathcal{X})$  is considered as the function of fusion. In the Eq. (1), multi-modality fusion can be studied in two aspects: input variable, i.e., input features, and fusion functions. Therefore, following the idea of Eq. (1), the previously published studies can be also divided into two categories, one focused on the input features (“macro” level), and the other focused on constructing the fusion functions (“micro” level).

**Macro level.** This type of paper is aimed to solve the problem of where to fuse, that is, which stage of the input features to choose to fuse. Most of them always explore the best fusion stage by designing the macro network architectures. The first study of this type [20] investigates two deep fusion architectures (early fusion and late fusion) and analyzes their performance on multispectral data. To further explore the potential of deep models for multispectral pedestrian detection, Liu et al. [1] carefully design another two ConvNet fusion architectures (halfway fusion and score fusion), and demonstrate that the halfway fusion model achieved the best detection synergy. Since then, several subsequent work [3, 4, 7, 21] has illustrated that the halfway fusion is overwhelmingly outperforming than other three fusion architectures.

**Mirco level.** Besides the macro network architectures, the construction of fusion function is another point for complementary learning of modality interaction. Naturally, the most straightforward way is to utilize concatenation, element-wise addition, element-wise average/maximum, and element-wise cross product to direct fuse feature maps of RGB and Thermal modalities. Two variations of novel Gated Fusion Units (GFU) [22] are proposed in GFD-SSD to learn the combination of feature maps generated by the two SSD middle layers. Zhang et. al. [6] propose a novel cycle fuse-and-refine module to improve the multispectral feature fusion while taking into account the complementary/consistency balance of the features. Different from the prior methods, we suggest a transformer-based scheme to carry out intra-modal and inter-modal information fusion with the help of self attention.

## III. PROPOSED METHOD

**Overview.** To demonstrate the effectiveness of our proposed CFT fusion module, we extend the framework of YOLOv5<sup>1</sup>,

to enable multispectral object detection. To be precise, we redesign the YOLOv5 feature extraction network to become a two-stream backbone, and embedded the CFT modules to facilitate modal fusion and modal interaction, named as *Cross-Modality Fusion Backbone*. An illustration of our *Cross-Modality Fusion Backbone* and *Cross-Modality Fusion Transformer* is presented in Fig. 2.

**Formulated details.** Specifically, given the intermediate RGB convolution feature maps  $\mathbf{F}_R \in \mathbb{R}^{C \times H \times W}$ , and thermal convolution feature maps  $\mathbf{F}_T \in \mathbb{R}^{C \times H \times W}$ , the sentences  $\mathbf{I}_R \in \mathbb{R}^{HW \times C}$  and  $\mathbf{I}_T \in \mathbb{R}^{HW \times C}$  are obtained by flattening each feature map and permuting the order of the matrices. Second, we concatenate the sentences of each modality and add a learnable positional embedding, which is a trainable parameter of dimension  $2HW \times C$ , to get the input sentences  $\mathbf{I} \in \mathbb{R}^{2HW \times C}$  of the transformer. The positional embedding enables the model to discriminate spatial information between different tokens at train time. Third, the input sequence  $\mathbf{I}$  is projected onto three weight matrices to compute a set of queries, keys and values ( $\mathbf{Q}$ ,  $\mathbf{K}$  and  $\mathbf{V}$ ),

$$\mathbf{Q} = \mathbf{I}\mathbf{W}^Q, \quad (2)$$

$$\mathbf{K} = \mathbf{I}\mathbf{W}^K, \quad (3)$$

$$\mathbf{V} = \mathbf{I}\mathbf{W}^V, \quad (4)$$

where  $\mathbf{W}^Q \in \mathbb{R}^{C \times D_Q}$ ,  $\mathbf{W}^K \in \mathbb{R}^{C \times D_K}$  and  $\mathbf{W}^V \in \mathbb{R}^{C \times D_V}$  are weight matrices. Moreover,  $D_Q$ ,  $D_K$  and  $D_V$  are equal in our transformer, i.e.,  $D_Q = D_K = D_V = 2HW$ . Fourth, the self attention layer uses the scaled dot products between  $\mathbf{Q}$  and  $\mathbf{K}$  to compute the attention weights and then multiply by the values to infer the refined output  $\mathbf{Z}$ ,

$$\mathbf{Z} = \text{Attention}(\mathbf{Q}, \mathbf{K}, \mathbf{V}) = \text{softmax}\left(\frac{\mathbf{Q}\mathbf{K}^T}{\sqrt{D_Q}}\right)\mathbf{V}, \quad (5)$$

where  $\frac{1}{\sqrt{D_Q}}$  is a scaling factor for preventing the softmax function from converging to a region with extremely small gradients when the magnitude of dot products grow large. To encapsulate multiple complex relationships from different representation subspaces at different positions, the multi-head attention mechanism is adopted,

$$\begin{aligned} \mathbf{Z}' &= \text{MultiHead}(\mathbf{Q}, \mathbf{K}, \mathbf{V}) = \text{Concat}(\mathbf{Z}_1, \dots, \mathbf{Z}_h)\mathbf{W}^O, \\ \mathbf{Z}_i &= \text{Attention}\left(\mathbf{Q}\mathbf{W}_i^Q, \mathbf{K}\mathbf{W}_i^K, \mathbf{V}\mathbf{W}_i^V\right). \end{aligned} \quad (6)$$

The subscript  $h$  denotes the number of heads, and  $\mathbf{W}^O \in \mathbb{R}^{h \cdot C \times 2HW}$  denotes the projected matrix of  $\text{Concat}(\mathbf{Z}_1, \dots, \mathbf{Z}_h)$ . Then the transformer uses a non-linear transformation to calculate the output sequences  $\mathbf{O}$ , which are of the same shape as input sequences  $\mathbf{I}$ ,

$$\mathbf{O} = \text{MLP}(\mathbf{Z}'') + \mathbf{Z}'', \quad (7)$$

where  $\mathbf{Z}'' = \mathbf{Z}' + \mathbf{I}$ . Finally, exploiting the inverse operation of the first step, the output sentences  $\mathbf{O}$  are converted into the recalibration results  $\mathbf{F}'_R$  and  $\mathbf{F}'_T$  and add to the original modality branch as complementary information.

<sup>1</sup>It is available at <https://github.com/ultralytics/yolov5>.

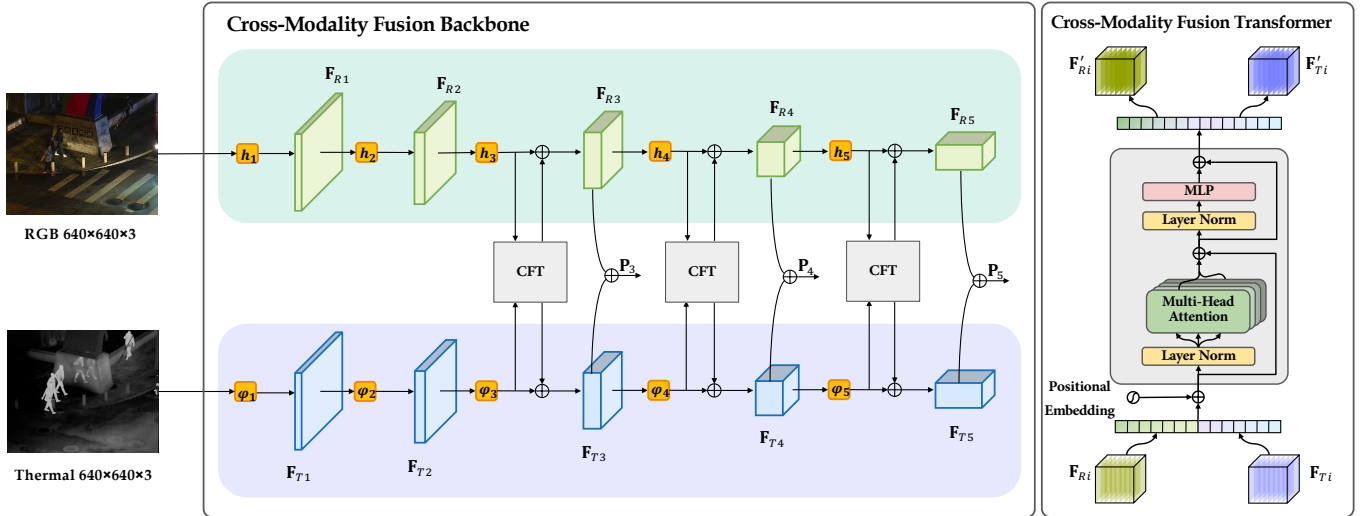


Fig. 2. Overview framework of Cross-Modality Fusion Backbone. The backbone consists of two parts: a two-stream feature extraction network and a Cross-Modality Fusion Transformer module. Among them,  $h_i$  and  $\varphi_i$  are the convolution modules of the RGB and Thermal branches,  $F_{R_i}$  and  $F_{T_i}$  are the feature maps of their respective modalities, and  $P_i$  represents the input of the feature pyramid.

**Implementation details.** The parameter amount and computational complexity of a standard transformer block can be formalized as

$$\text{Params} \sim O(\text{Transformer}) = 4HWC + 8C^2, \quad (8)$$

$$\text{FLOPs} \sim \Omega(\text{Transformer}) = 12HWC^2 + 2(HW)^2C. \quad (9)$$

And a CFT module has 8 duplicate transformer blocks, as shown in Fig. 2. In addition, since the dimension of the input sentences  $\mathbf{I}$  is  $2HW \times C$ , the actual expression of  $HW$  in the above Eq.(8) and (9) is  $2HW$ . Apart from the Parameters and FLOPs, the memory access also needs to be considered [23], especially when calculating the dot product of queries and keys, a correlation matrix of  $2HW \times 2HW$  dimensions will be generated. When the input picture size is  $640 \times 640$ , after two downsamplings ( $H = W = 160$ ), the elements of one correlation matrix  $\mathbf{QK}^T$  exceed 2.4G, which is unacceptable for ordinary computers.

For the sake of reducing expensive computation, our solution is to use a global average pooling that downsamples the feature maps to a low and fixed resolution of  $H = W = 8$  before passing them to the transformer block. And the output is upsampled by bilinear interpolation to the original resolution before being added to the original mode branch.

**Why transformer?** The main idea behind our module is leveraging the self attention mechanism to learn the binary relationship of RGB and Thermal modalities. As illustrated in Fig. 3, when calculating the correlation matrix  $\mathbf{QK}^T$ , four matrix blocks can be inferred, which are two intra-modality correlation matrix blocks (RGB and Thermal), and two inter-modality correlation matrix blocks. Hence, with the help of transformer, we don't need to carefully design the modal fusion module. We just only needs to simply splice the multi-modal features into a sequence, and then the transformer can automatically perform simultaneous intra-modality and inter-modality information fusion and robustly capture the latent interactions between RGB and Thermal domains.

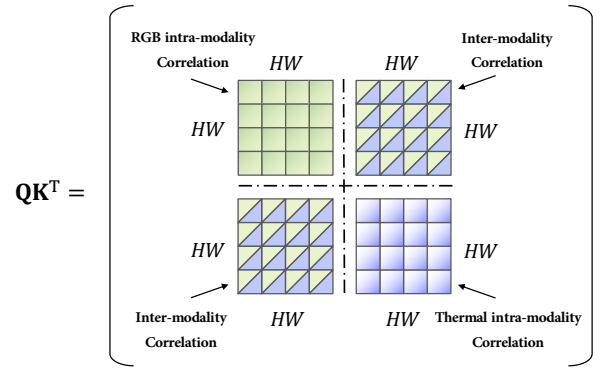


Fig. 3. Illustration of the correlation matrix  $\mathbf{QK}^T$ .

## IV. EXPERIMENT

### A. Datas

**FILP.** The FLIR ADAS dataset [10] is a challenging multispectral object detection dataset which includes day and night scenes. There are a lot of unaligned image pairs in the original data set, which makes network training difficult. Therefore, an “aligned” version [6] is recently released that manually removes unaligned visible-thermal image pairs. This new dataset contains 5,142 well-aligned multispectral image pairs, of which 4,129 pairs are used for training and 1,013 pairs are used for testing and cover three object categories: “person”, “car” and “bicycle”.

**LLVIP.** LLVIP [11] is a very recently released visible-infrared paired pedestrians dataset for low-light vision. This dataset contains 33672 images, or 16836 pairs, most of which were taken at very dark scenes, and all of the images are strictly Spatio-temporal aligned.

**VEDAI.** In addition to the above two ground-view datasets, we also test our method on VEDAI which is a multispec-

tral aerial imagery dataset for vehicle detection. The dataset contains nine vehicle classes for a total of more than 3700 annotated targets in more than 1200 images in each resolution (1024 × 1024 and 512 × 512).

*B. Training Details*

In these experiments, YOLOv5 is chosen as our base detector. By adding an additional branch for the extraction of thermal features, it is transformed into a two-stream convolutional neural network, as illustrated in Fig. 2. We use SGD optimizer with an initial learning rate of 1e-2, a momentum of 0.937, and a weight decay of 0.0005. As for data augmentation, we use the Mosaic method which mixes four training images in one image.

*C. Ablation Study*

All models are evaluated with three usual object detection metrics introduced with MS-COCO: mAP50, mAP75, and mAP. The best records and the improvements are marked in bold and ↑, respectively. We compare in Table I the detection performance with and without CFT on different datasets (FLIR, LLVIP, and VEDAI). And the results confirm that our CFT has general significance for improving the performance of multispectral object detection.

TABLE I  
ABLATION EXPERIMENTS ON THREE DATASETS

Dataset	CFT	mAP50	mAP75	mAP
FLIR		73.0	32.0	37.4
	✓	<b>77.7</b> (↑4.7)	<b>34.8</b> (↑2.8)	<b>40.0</b> (↑2.6)
LLVIP		95.8	71.4	62.3
	✓	<b>97.5</b> (↑1.7)	<b>72.9</b> (↑1.5)	<b>63.6</b> (↑1.3)
VEDAI		79.7	47.7	46.8
	✓	<b>85.3</b> (↑5.6)	<b>65.9</b> (↑8.2)	<b>56.0</b> (↑9.2)

*D. Comparison with State-of-the-art Methods*

**On FLIR.** Tabel II reports the experimental results of our approach and other methods for comparison. It can be observed that our CFT achieves state-of-the-art performance on this dataset. Furthermore, it wins with an overwhelming advantage, and the gap between CFT and others is at least 4.8%, and up to 6.5% on mAP50. Even compared to the latest GAFF [7], our method outperforms 4.8%, 1.9%, and 2.5% on mAP50, mAP75, and mAP respectively, which is a significant improvement on this dataset.

TABLE II  
COMPARISON ON FILR DATASET

Model	Data	Backbone	mAP50	mAP75	mAP
halfway fusion [6]	RGB+IR	VGG16	71.2	-	-
CFR_3 [6]	RGB+IR	VGG16	72.4	-	-
GAFF [7]	RGB+IR	ResNet18	72.9	32.9	37.5
GAFF [7]	RGB+IR	VGG16	72.7	30.9	37.3
CFT(Ours)	RGB+IR	CFB	<b>77.7</b>	<b>34.8</b>	<b>40.0</b>

**On LLVIP.** Table III presents the detection results of CFT and other mono-modality networks, especially YOLOv5 which

is the basis of our algorithm, on the LLVIP dataset. What stands out in the table (below) is that a more accurate detection (mAP50:97.5, mAP75:72.9, mAP:63.6) can be pushed by fusing the complementary features of different modalities based on the transformer.

TABLE III  
COMPARISON ON LLVIP DATASETS

Model	Data	Backbone	mAP50	mAP75	mAP
mono-modality networks					
YOLOv3 [11]	RGB	Darknet53	85.9	37.9	43.3
YOLOv3 [11]	IR	Darknet53	89.7	53.4	52.8
YOLOv5 [11]	RGB	CSPDarknet53	90.8	51.9	50.0
YOLOv5 [11]	IR	CSPDarknet53	94.6	72.2	61.9
multi-modality networks					
CFT(Ours)	RGB+IR	CFB	<b>97.5</b>	<b>72.9</b>	<b>63.6</b>

**On VEDAI.** As mentioned before, the multispectral aerial imagery dataset VEDAI is used in this experiment. Again, we can observe from Table IV that our method brings very impressive gains for all the considered evaluation metrics (mAP50:↑9.3, mAP:↑10.0).

TABLE IV  
COMPARISON ON VEDAI DATASETS

Model	Data	Backbone	mAP50	mAP
mono-modality networks				
Retina [25]	RGB	ResNet-50	-	43.5
Faster R-CNN [16]	RGB	ResNet-101	-	34.8
SSSDet [27]	RGB	shallow network	-	46.0
SSD [17]	RGB	VGG16	70.9	-
SSD [17]	IR	VGG16	69.8	-
EfficientDet(D1) [26]	RGB	EfficientNet(B1)	74.0	-
EfficientDet(D1) [26]	IR	EfficientNet(B1)	71.2	-
YOLO-fine [28]	RGB	Darknet53	76.0	-
YOLO-fine [28]	IR	Darknet53	75.2	-
multi-modality networks				
YOLOv3 early fusion [24]	RGB+IR	Darknet53	-	44.0
YOLOv3 mid fusion [24]	RGB+IR	Darknet53	-	44.6
CFT(ours)	RGB+IR	CFB	<b>85.3</b>	<b>56.0</b>

V. CONCLUSION

In this work, we propose a novel transformer-based fusion approach, named Cross-Modality Fusion Transformer (CFT), to enhance the representation capability of two-stream CNNs in multispectral object detection. More specifically, the CFT modules are densely inserted in the backbone to integrate features, so the inherent complementary between different modalities can be fully exploited. Moreover, we derive the process of how the CFT module fuses the multi-modality feature maps from the formula and implementation view. Extensive experiments demonstrate that our proposed method can achieve the state-of-the-art performance. Given that our approach is simple yet effective, it may do a favor to other computer vision fields such as RGB-LiDAR, RGB-D, stereo image SR tasks, etc.

## REFERENCES

- [1] Liu, J., Zhang, S., Wang, S., and Metaxas, D. N., "Multispectral deep neural networks for pedestrian detection," *Br. Mach. Vis. Conf.*, pp.73.1-73.13, Sep. 2016, doi: 10.5244/C.30.73.
- [2] Park, K., Kim, S., and Sohn, K., "Unified multi-spectral pedestrian detection based on probabilistic fusion networks," *Pattern Recognit.*, vol. 80, pp.143-155, 2018, doi: 10.1016/j.patcog.2018.03.007.
- [3] Li, C., Song, D., Tong, R., and Tang, M. "Multispectral pedestrian detection via simultaneous detection and segmentation". *Br. Mach. Vis. Conf.*, Sep. 2018, pp.225.1-225.12, 2018.
- [4] Li, C., Song, D., Tong, R., and Tang, M. "Illumination-aware faster R-CNN for robust multispectral pedestrian detection," *Pattern Recognit.*, vol.85, pp.161-171, 2019, doi:10.1016/j.patcog.2018.08.005.
- [5] Zhang, L., Liu, Z., Zhang, S., Yang, X., Qiao, H., Huang, K., and Hussain, A., "Cross-modality interactive attention network for multispectral pedestrian detection," *Inf. Fusion*, vol.50, pp.20-29, 2019.
- [6] H. Zhang, E. Fromont, S. Lefevre and B. Avignon, "Multispectral fusion for object detection with cyclic fuse-and-refine blocks," *Int. Conf. Image Process*, pp. 276-280, 2020, doi: 10.1109/ICIP40778.2020.9191080.
- [7] H. Zhang, E. Fromont, S. Lefevre and B. Avignon, "Guided attentive feature fusion for multispectral pedestrian detection," *IEEE Winter Conf. Appl. Comput. Vis.*, pp. 72-80, 2021, doi: 10.1109/WACV48630.2021.00012.
- [8] Chen, Y. T., Shi, J., Mertz, C., Kong, S., and Ramanan, D., "Multimodal Object Detection via Bayesian Fusion," *arXiv preprint*, arXiv:2104.02904.
- [9] Sharma, M., Dhanaraj, M., Karnam, S., Chachlakis, D. G., Ptucha, R., Markopoulos, P. P., and Saber, E., "YOLOrs: Object detection in multimodal remote sensing imagery," *IEEE J. Sel. Top. Appl. Earth Obs. Remote Sens.*, vol. 14, pp. 1497-1508, 2021, doi: 10.1109/JS-TARS.2020.3041316.
- [10] "Free flir thermal dataset for algorithm training," [Online]. Available: <https://www.flir.com/oem/adas/adas-dataset-form/>.
- [11] Jia, X., Zhu, C., Li, M., Tang, W., and Zhou, W., "LLVIP: A visible-infrared paired dataset for low-light vision," *IEEE Int. Conf. Comput. Vis. Workshops*, pp. 3496-3504, 2021.
- [12] Razakarivony, S., and Jurie, F. "Vehicle detection in aerial imagery: A small target detection benchmark," *J. Vis. Commun. Image R.*, vol. 34, pp.187-203, 2016.
- [13] Krizhevsky, A., Sutskever, I., and Hinton, G. E., "Imagenet classification with deep convolutional neural networks," *Adv. Neural Inf. Proces. Syst.*, vol. 25, pp.1097-1105, 2012.
- [14] He, K., Zhang, X., Ren, S., and Sun, J., "Deep residual learning for image recognition," *IEEE Conf. Comput. Vis. Pattern Recognit.*, pp. 770-778, 2016.
- [15] R. Girshick, J. Donahue, T. Darrell and J. Malik, "Rich Feature Hierarchies for Accurate Object Detection and Semantic Segmentation," *IEEE Conf. Comput. Vis. Pattern Recognit.*, pp. 580-587, 2014, doi: 10.1109/CVPR.2014.81.
- [16] S. Ren, K. He, R. Girshick and J. Sun, "Faster R-CNN: Towards Real-Time Object Detection with Region Proposal Networks," *IEEE Trans. Pattern Anal. Mach. Intell.*, vol. 39, no. 6, pp. 1137-1149, 1 June 2017, doi: 10.1109/TPAMI.2016.2577031.
- [17] Liu, W., Anguelov, D., Erhan, D., Szegedy, C., Reed, S., Fu, C. Y., and Berg, A. C., "Ssd: Single shot multibox detector," *Eur. Conf. Comput. Vis.*, pp. 21-37, Oct., 2016, doi:10.1007/978-3-030-58452-8\_1.
- [18] J. Redmon, S. Divvala, R. Girshick and A. Farhadi, "You Only Look Once: Unified, Real-Time Object Detection," *IEEE Conf. Comput. Vis. Pattern Recognit.*, pp. 779-788, 2016, doi: 10.1109/CVPR.2016.91.
- [19] Vaswani, A., Shazeer, N., Parmar, N., Uszkoreit, J., Jones, L., Gomez, A. N., Kaiser, L. and Polosukhin, I., "Attention is all you need," *Adv. Neural Inf. Proces. Syst.*, pp. 5998-6008, 2017.
- [20] Wagner, J., Fischer, V., Herman, M., and Behnke, S., "Multispectral Pedestrian Detection using Deep Fusion Convolutional Neural Networks," *Euro. Symp. Artif. Neural Networks, Comput. Intell. Mach. Learn.*, Vol. 587, pp. 509-514, Apr., 2016.
- [21] L. Zhang, X. Zhu, X. Chen, X. Yang, Z. Lei and Z. Liu, "Weakly Aligned Cross-Modal Learning for Multispectral Pedestrian Detection," *IEEE Int. Conf. Comput. Vis.*, pp. 5126-5136, 2019, doi: 10.1109/ICCV.2019.00523.
- [22] Zheng, Y., Izzat, I. H., and Ziaee, S. (2019). "GFD-SSD: gated fusion double SSD for multispectral pedestrian detection," *arXiv preprint*, arXiv:1903.06999.
- [23] Ma, N., Zhang, X., Zheng, H. T., and Sun, J., "Shufflenet v2: Practical guidelines for efficient cnn architecture design," *Euro. Conf. Comput. Vis.*, pp. 116-131, 2018.
- [24] Dhanaraj, M., Sharma, M., Sarkar, T., Karnam, S., Chachlakis, D. G., Ptucha, R., Markopoulos P. P. and Saber, E., "Vehicle detection from multi-modal aerial imagery using YOLOv3 with mid-level fusion," *Proc. SPIE, Big Data II: Learning, Analytics, and Applications*, Vol.11395, May, 2020, doi:10.1117/12.2558115.
- [25] T. Lin, P. Goyal, R. Girshick, K. He and P. Dollár, "Focal Loss for Dense Object Detection," *IEEE Trans. Pattern Anal. Mach. Intell.*, vol. 42, no. 2, pp. 318-327, 1 Feb. 2020, doi: 10.1109/TPAMI.2018.2858826.
- [26] M. Tan, R. Pang and Q. V. Le, "EfficientDet: Scalable and Efficient Object Detection," *IEEE Conf. Comput. Vis. Pattern Recognit.*, pp. 10778-10787, 2020, doi: 10.1109/CVPR42600.2020.01079.
- [27] M. Mandal, M. Shah, P. Meena and S. K. Vipparthi, "SSSDet: Simple Short and Shallow Network for Resource Efficient Vehicle Detection in Aerial Scenes," *Int. Conf. Image Process*, pp. 3098-3102, 2019, doi: 10.1109/ICIP.2019.8803262.
- [28] Pham, M. T., Courtrai, L., Friguet, C., Lefèvre, S., and Baussard, A., "YOLO-Fine: one-stage detector of small objects under various backgrounds in remote sensing images," *Remote Sens.*, 12(15), 2501, 2020.